A&A 408, 1057–1063 (2003)
DOI: 10.1051/0004-6361:20031028

Astronomy & Astrophysics

Diagnostics of the plasma of pulsar magnetospheres based on polarization profiles of radio pulses

S. A. Petrova⋆

Institute of Radio Astronomy, 4, Chervonopraporna St., Kharkov 61002, Ukraine

Received 30 April 2003 / Accepted 3 June 2003

Abstract. Propagation of natural waves through the ultrarelativistic highly magnetized plasma in the rotating magnetosphere of a pulsar is considered. Based on the quantitative description of the polarization-limiting effect, we develop a technique of density diagnostics of pulsar plasma according to the observed polarization profiles of radio pulses. For the first time, it appears possible to obtain the profiles of the plasma density distribution across the open field line tube. The density profiles found for PSR B0355+54 and PSR B0628-28 show a perfect exponential decrease towards the tube edge. The multiplicity factors derived are compatible with those predicted by modern theories of pair cascade in pulsars. The results of the plasma density diagnostics may have numerous implications for the physics of the pulsar magnetosphere. Further application of the suggested technique to single-pulse polarization data seems to be promising.

Key words. plasmas – polarization – waves – stars: pulsars: general – stars: pulsars: individual: PSR B0355+54, PSR B0628-28

1. Introduction

Pulsar magnetospheres are believed to contain an ultrarelativistic secondary plasma which streams along the open magnetic lines. Narrowness of the observed pulses implies that the radio emission originates deep inside the magnetosphere. Further on, the waves propagate through the plasma flow and their characteristics can be considerably changed by the ambient medium. Thus, the outgoing radiation can bear valuable information about the physical properties of pulsar plasma. In the present paper we suggest a way of finding the distribution of the number density of pulsar plasma based on the observed polarization characteristics of radio pulses.

The diverse and complicated behaviour of the single pulse polarization is mainly caused by the presence of orthogonal polarization modes (OPMs), which are fundamental feature of pulsar radiation. The concept of completely polarized superposed OPMs has strong observational support (McKinnon & Stinebring 1998, 2000) and it is undoubtedly favoured by theoretical considerations, since direct generation and further propagation of the partially polarized disjoint modes are questionable. The superposed modes can be recognized as the independently propagating natural waves of pulsar plasma, which either are generated by different emission mechanisms (McKinnon 1997) or originate as a result of partial conversion of a single emission mode (Petrova 2001). As the magnetic field of a pulsar is extremely strong and ray propagation is typically quasi-transverse, the natural waves of the magnetospheric plasma should be linearly polarized, with the electric vector reflecting the orientation of the ambient magnetic field. However, the representation of the observed superposed OPMs as the natural waves of pulsar plasma faces two major difficulties. Firstly, the observed modes are elliptically polarized, with the degree of circular polarization varying stochastically from pulse to pulse (McKinnon 2002). Secondly, at a fixed pulse longitude, for each of the orthogonal states there is a substantial pulse-to-pulse spread in position angle (PA) of linear polarization (McKinnon & Stinebring 1998), and moreover, the average PAs of the two states may differ by not exactly 90° (e.g. Gil et al. 1991, 1992).

From the theoretical point of view, if one consistently considers propagation of natural waves in the open field line tube of a pulsar, one cannot overlook the region where the waves decouple from the magnetospheric plasma and become common vacuum electromagnetic waves. This happens as soon as the plasma density decreases sufficiently for the approximation of geometrical optics to be broken, i.e. on condition that

$$\frac{\omega}{c} r \Delta n(N, \gamma, \theta, \omega) \sim 1, \tag{1}$$

where Δn is the difference in the refractive indices of the modes, N and γ are the number density and Lorentz-factor of the plasma, θ is the angle between the wavevector and the ambient magnetic field. Before the natural waves escape from pulsar plasma, their polarization can be substantially altered. In the region defined by the above equation the waves acquire some circular polarization and a shift in PA with respect to the orientation of the ambient magnetic field. This effect, usually called the "polarization-limiting effect" (PLE), has been qualitatively considered by Cheng & Ruderman (1979), Stinebring (1982)

⋆ e-mail: rai@ira.kharkov.ua

and Barnard (1986) and later on quantitatively described in Lyubarskii & Petrova (1999) and Petrova & Lyubarskii (2000). For fixed parameters of the plasma, both natural waves have the same PA shift and the same degree of circular polarization (of opposite senses), becoming purely orthogonal elliptical waves (Petrova 2001). It is important to note that the values of PA shift and mode ellipticity resulting from PLE are related to each other, both being determined by the physical conditions in the polarization-limiting region. Then the observed pulse-to-pulse variations of these quantities can naturally be attributed to fluctuations in pulsar plasma. On the one hand, PLE allows one to correctly account for the mode ellipticity and PA spread, improving the theory of formation of pulsar polarization. On the other hand, it provides the possibility of plasma diagnostics based on polarization data.

In the present paper, we develop a technique that allows us to separate the observational consequences of PLE from the polarization data and to obtain the plasma number density profiles. The technique is applied to the average polarization profiles of PSR B0355+54 (at 4.85 GHz) and PSR B0628-28 (at 0.408 and 0.61 GHz), where the contribution of pulse-to-pulse orthogonal transitions is believed to be negligible, so that the average polarization characteristics can be regarded as those of a "typical" single pulse. Although our results are rather illustrative, they do encourage further application of the suggested technique to real single pulses of a variety of pulsars, in which case the orthogonal transitions and other pulse-to-pulse polarization fluctuations can be properly taken into account. Our present research has made use of the database of published pulse profiles maintained by the European Pulsar Network, available at `http://www.mpifr-bonn.mpg.de/pulsar/data`.

2. General equations

Let us consider radio wave propagation through an ultrarelativistic highly magnetized plasma in the rotating pulsar magnetosphere. The plasma particles are known to stream along the magnetic lines with a large spread in Lorentz-factors, $\gamma \sim 10$–100. However, the dispersive properties of the plasma are mainly determined by the particles with momenta close to some characteristic value (e.g. Lyubarskii 1996), so that the cold plasma approximation is still appropriate for our problem. Deep inside the magnetosphere, pulsar plasma allows two nondamping natural waves, the ordinary and extraordinary ones, which are linearly polarized. The electric vector of the ordinary wave lies in the same plane as the wavevector and the ambient magnetic field, while the extraordinary wave is polarized perpendicularly to this plane. The evolution of the electric field amplitudes of the waves is described by Eqs. (2.8) in Lyubarskii & Petrova (1999) (or Eqs. (13) in Petrova & Lyubarskii 2000). In terms of the Stokes parameters of the wave, those equations are reduced to the form:

$$\begin{aligned}\frac{\mathrm{d}q}{\mathrm{d}z} &= -2R(b_x+l_y)(b_y-l_x)v,\\ \frac{\mathrm{d}u}{\mathrm{d}z} &= R[(b_x+l_y)^2-(b_y-l_x)^2]v,\\ \frac{\mathrm{d}v}{\mathrm{d}z} &= 2R(b_x+l_y)(b_y-l_x)q+R[(b_y-l_x)^2-(b_x+l_y)^2]u,\end{aligned} \tag{2}$$

where $R = 2\omega_\mathrm{p}^2/\{\omega c\gamma^3[(b_x+l_y)^2+(b_y-l_x)^2]^2\}$, $\omega_\mathrm{p} = \sqrt{4\pi Ne^2/m}$ is the plasma frequency, b_x and b_y are the direction cosines of the ambient magnetic field in the Cartesian coordinate system with the z-axis along the wavevector, $\boldsymbol{l} = \boldsymbol{b}\times(\boldsymbol{\Omega}\times\boldsymbol{r})/c$ is the vector allowing for rotational aberration, $\boldsymbol{\Omega}$ is the angular velocity of pulsar rotation. Note that $q^2+u^2+v^2 \equiv 1$, since the natural waves are by definition completely polarized.

The Stokes parameters evolve along the wave trajectory because of the plasma density decrease, $N \propto z^{-3}$, and also because of variation of the orientation of the ambient magnetic field as a result of ray propagation and pulsar rotation. For the wave propagation far enough from the emission region, to the first order in z/r_L (where $r_\mathrm{L} = c/\Omega$ is the light cylinder radius) the geometrical terms can be presented as (for more details see e.g. Petrova & Lyubarskii 2000):

$$\begin{aligned}b_x+l_y &= \frac{\theta}{2}-\frac{z}{2r_\mathrm{L}}\frac{\Phi\sin^2\alpha}{\theta},\\ b_y-l_x &= \frac{z}{2r_\mathrm{L}}\frac{\xi-\alpha}{\theta}\sin\alpha,\end{aligned} \tag{3}$$

where θ is the wavevector's tilt to the magnetic axis, Φ the pulse phase, $\Phi^2\sin^2\alpha = \theta^2-(\xi-\alpha)^2$, α is the angle between the rotational and magnetic axes, ξ the angle between the rotational axis and the sight line; $|\xi-\alpha|, \theta, |\Phi| \ll 1$. In the chosen coordinate system, $\boldsymbol{b}$ initially lies in the xz-plane, so that the initial conditions read: $q_0 = \pm 1$, $u_0 = v_0 = 0$, where the sign "+" refers to the ordinary waves and the sign "−" to the extraordinary ones.

Substituting Eq. (3) into Eq. (2), we find finally:

$$\begin{aligned}\frac{\mathrm{d}q}{\mathrm{d}w} &= -2\rho G_2(w-\rho G_1)Av,\\ \frac{\mathrm{d}u}{\mathrm{d}w} &= [(w-\rho G_1)^2-(\rho G_2)^2]Av,\\ \frac{\mathrm{d}v}{\mathrm{d}w} &= 2\rho G_2(w-\rho G_1)Aq+[(\rho G_2)^2-(w-\rho G_1)^2]Au.\end{aligned} \tag{4}$$

Here $w = z_\mathrm{p}/z$, z_p is the polarization-limiting radius defined by the following relation (cf. Eq. (1)):

$$R(z_\mathrm{p})z_\mathrm{p}[(b_x+l_y)^2+(b_y-l_x)^2]_{z_\mathrm{p}} = 1; \tag{5}$$

$$\begin{aligned}A &= \frac{w^3[(1-\rho G_1)^2+(\rho G_2)^2]}{[(w-\rho G_1)^2+(\rho G_2)^2]^2}, \quad \rho = \frac{z_\mathrm{p}}{r_\mathrm{L}}\frac{\sin\alpha}{|\xi-\alpha|},\\ \eta &= \frac{\Phi\sin\alpha}{\xi-\alpha}, \quad G_1 = \frac{\eta}{1+\eta^2}, \quad G_2 = \frac{\mathrm{sign}(\xi-\alpha)}{1+\eta^2}.\end{aligned}$$

As can be seen from Eq. (4), polarization evolution of the natural waves is completely determined by the two parameters, ρ and η. The first contains the polarization-limiting radius and, consequently, is related to the plasma number density at z_p (see Eq. (5)). As for the second parameter, $\eta \approx -\tan\psi_0$, where ψ_0 can be recognized as the position angle in the customary rotating-vector model (RVM) (e.g. Manchester & Taylor 1977). As usual, ψ_0 corresponds to the PA of the natural wave in

the emission region, i.e. in our case represents the angle between the xz-plane and the $\boldsymbol{k} \times \boldsymbol{\Omega}$-plane. The minus sign in the above relation allows for the so-called "ψ-convention problem" (e.g. Everett & Weisberg 2001), since throughout the paper we follow the usual astronomical convention that PA increases counter-clockwise on the sky.

The solution of the set of Eq. (4) at $z \gg z_p$ yields the final polarization of the natural waves. Below we are interested in the final degree of circular polarization, v_∞, and the final PA shift from the initial plane of magnetic lines, $\Delta\psi_\infty = \frac{1}{2}\arctan(u_\infty/q_\infty)$. Figure 1 shows the numerically calculated final polarization characteristics of the ordinary waves as functions of the parameters η and ρ. According to Fig. 1c, the pairs (η, ρ) and $(v_\infty, \Delta\psi_\infty)$ exhibit a unique correspondence.

Both polarization characteristics of the natural waves, v_∞ and $\Delta\psi_\infty$, can be derived from observations. Given that the observed radiation is an incoherent mixture of the orthogonal elliptical modes with intensities I_1 and I_2, the observed Stokes parameters (I, Q, U, V) are written as

$$I = I_1 + I_2, \quad L = l_m(I_1 - I_2),$$
$$V = v_m(I_1 - I_2),$$

where $L = \sqrt{Q^2 + U^2}$ is the observed linear polarization, l_m and v_m correspond to the degree of linear and circular polarization of the modes, $l_m^2 + v_m^2 = 1$. For the dominant mode we have:

$$v_m = \frac{V}{\sqrt{L^2 + V^2}}, \quad \psi = \frac{1}{2}\arctan(U/Q). \tag{6}$$

On the other hand, if the observed superposed OPMs are identified with the natural waves which undergo PLE,

$$v_m = v_\infty, \quad \psi = \Delta\psi_\infty - \arctan\eta. \tag{7}$$

Because of the unique correspondence between the pairs $(v_\infty, \Delta\psi_\infty)$ and (η, ρ), the pair of the observed values (v_m, ψ) is unambiguously related to (η, ρ). With the values of η derived from (v_m, ψ) at different pulse longitudes, one can reconstruct a perfect RVM swing of PA and fit the geometrical parameter $\frac{\sin\alpha}{\xi-\alpha}$. Further on, substituting ρ and η into Eq. (5) yields the plasma number density at z_p. With the polarization data across the profile, one can find the plasma density at different distances to the magnetic axis. It appears possible to reconstruct the plasma density distribution over a substantial part of the tube.

3. Results

In the previous section, we have outlined the basic ideas underlying the suggested technique of density diagnostics of pulsar plasma. An example of its application to the observational data is demonstrated below. We use the average polarization profile of PSR B0355+54 at 4.85 GHz first published by von Hoensbroech & Xilouris (1997). Strictly speaking, our technique should be applied to the single-pulse data. Since the values of v_m and ψ can undergo marked pulse-to-pulse fluctuations – first of all, as a result of orthogonal transitions – the average polarization profiles are typically inappropriate. However, for the leading part of the profile considered one can expect the absence of orthogonal transitions and generally weak pulse-to-pulse polarization changes (e.g. Xilouris et al. 1995), with the average v_m and ψ still resembling the single-pulse values.

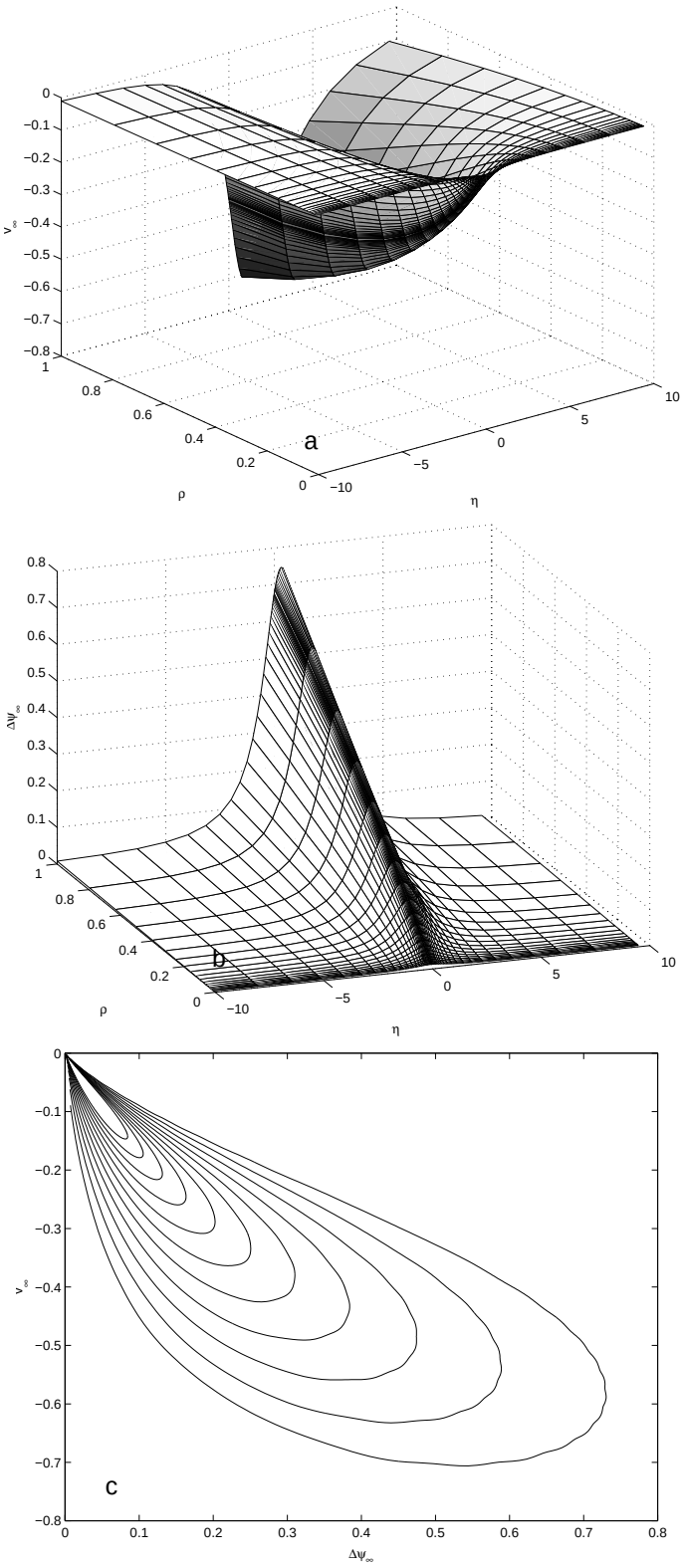

Fig. 1. The final ellipticity **a**) and PA shift **b**) of the ordinary waves as functions of parameters η and ρ; **c**) v_∞ versus $\Delta\psi_\infty$ at different (ρ, η), each of the closed lines corresponds to ρ = const.

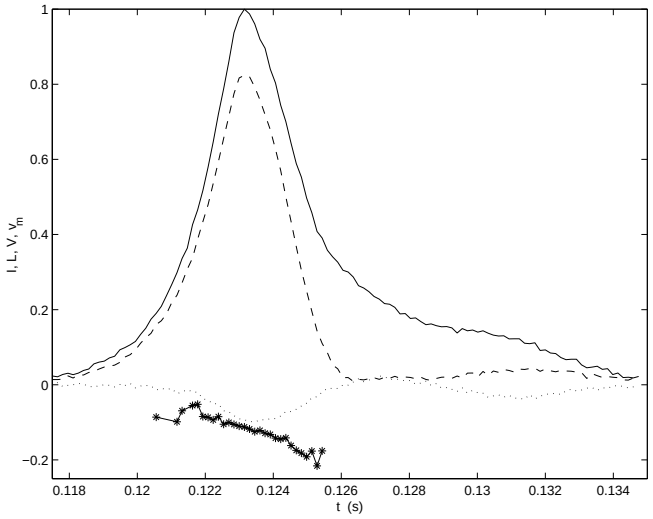

Fig. 2. Polarization profile of PSR B0355+54 at 4.85 GHz (von Hoensbroech & Xilouris 1997): solid line – total intensity, dashed line – linear polarization, dotted line – circular polarization, asterisks – reliable values of mode ellipticity.

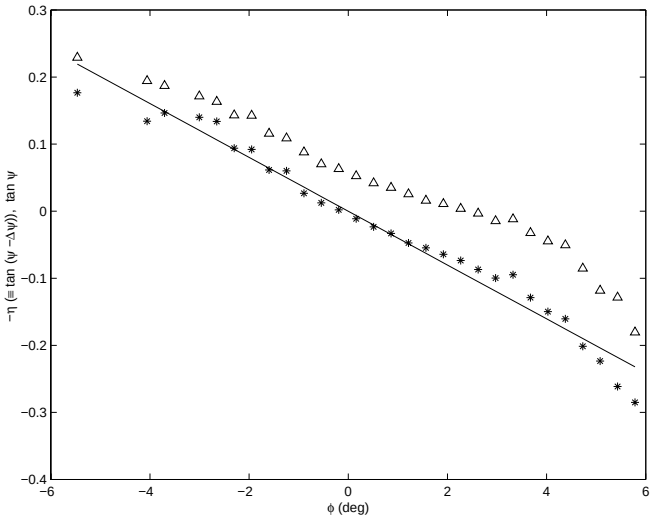

Fig. 3. Parameter $-\eta$ ($= \tan\psi_0 = \tan(\psi - \Delta\psi_\infty)$) versus pulse longitude (asterisks) according to the polarization data on PSR B0355+54 at 4.85 GHz; the observed values, $\tan\psi$, are shown by triangles.

The profile of PSR B0355+54 is plotted in Fig. 2. The reliable values of mode ellipticity, υ_m, calculated in accordance with Eq. (6) are shown by asterisks. The errors in υ_m are assumed to be normally distributed; hence, the standard error reads: $\sigma_{\upsilon_m} = \frac{\sqrt{(Q^2\sigma_Q^2+U^2\sigma_U^2)V^2+\sigma_V^2(Q^2+U^2)^2}}{(Q^2+U^2+V^2)^{3/2}}$, where $\sigma_{Q,U,V}$ are the rms-deviations of the Stokes parameters in the off-pulse region. Our consideration involves the points with the relative errors $\sigma_{\upsilon_m}/|\upsilon_m| \le 0.3$. The standard errors in PA, $\sigma_\psi = \frac{\sqrt{Q^2\sigma_U^2+U^2\sigma_Q^2}}{2(Q^2+U^2)}$, and the corresponding relative errors are typically much less.

For the pulse longitudes considered, the tangent of the observed PA is presented in Fig. 3 (triangles). According to the sign of the PA derivative, $\xi - \alpha > 0$. Then, as can be seen from Eq. (4) and Fig. 1, the negative sign of υ_m testifies to the dominance of the ordinary waves. Using the numerical solution of

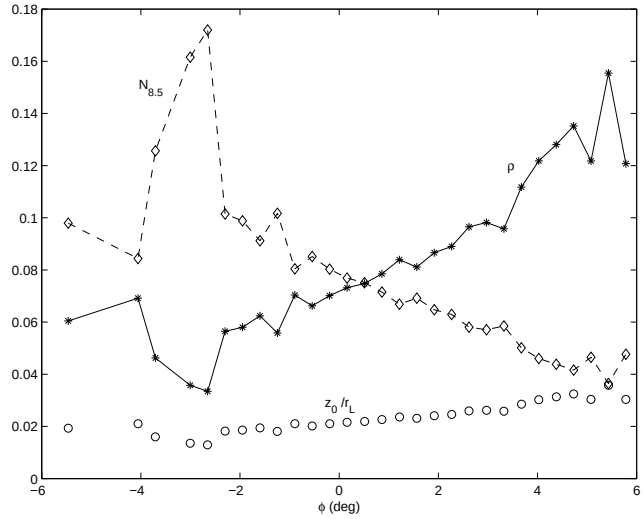

Fig. 4. Parameter ρ as function of pulse longitude (asterisks) for PSR B0355+54 at 4.85 GHz. The normalized plasma density at z_p estimated following Eq. (8) is shown by diamonds, $N_{8.5} = \frac{N_p}{3\times10^8}$ cm^{-3}. The emission altitude, z_0, found from the relation $\omega = \omega_p(z_0)\sqrt{\gamma}$ is shown by circles. For more details see text.

PLE-equations (4) at various ρ and η, for each pair of the observed values (υ_m, ψ) one can find a unique pair (η, ρ) which provides such values of υ_∞ and $\Delta\psi_\infty$ that satisfy both equalities (7) simultaneously. Figures 3 and 4 show the resultant η and ρ versus pulse longitude. The function $-\eta(\Phi)$ (asterisks in Fig. 3) indeed exhibits a monotonic behaviour and can be well fitted by a straight line. Obtained purely from the observed values $(\upsilon_m(\Phi), \psi(\Phi))$, this dependence appears compatible with the definition, $\eta = \Phi\frac{\sin\alpha}{\xi-\alpha}$, and presents a perfect RVM-swing of the initial PA, $\eta = -\tan\psi_0$, reflecting the magnetic field geometry in the emission region. This strongly supports joint interpretation of PA shift and the mode ellipticity in terms of PLE.

It should be mentioned that fitting the RVM-curve directly to the observed PA usually faces difficulties, even in the absence of prominent orthogonal transitions (e.g. Everett & Wiesberg 2001). Moreover, in those rare cases when the fitting procedure yields satisfactory results, the geometrical parameters of a pulsar derived from the fitted curves at different frequencies appear to differ drastically. Probably, these discrepancies can be attributed to PLE. Further on it would be reasonable to allow for this effect and fit the RVM-curve to ψ_0 rather than to ψ. Although in the case considered, ψ and ψ_0 differ slightly, in general one can expect that taking into account PLE can improve the technique of RVM-fits, especially in application to the single-pulse data.

According to the theory of PLE, the linearly polarized natural wave originating with the RVM position angle, $\psi_0 = -\arctan\eta$, acquires both the observed ψ and υ_m at a certain value of ρ, which characterizes the physical properties of the ambient plasma. The quantity ρ is related to the polarization-limiting radius, $\rho = Cz_p/r_L$, with $C = \sin\alpha/|\xi - \alpha| = |\eta/\phi|$. In our case $C = 2.3$, corresponding to the slope of a straight line in Fig. 3. Then $z_p/r_L \lesssim 0.1$ (cf. Fig. 4).

Proceeding from Eq. (5), one can find the plasma number density at z_p:

$$N_p = 1.5\times10^6 P^{-1}\nu_9\gamma_2^2(\xi-\alpha)^2 C\rho^{-1}(1+\eta^2) \times[(1-\rho G_1)^2+(\rho G_2)^2]\ \mathrm{cm}^{-3}, \quad (8)$$

where P is the pulsar period, ν the radio frequency, $\nu_9 = \frac{\nu}{10^9\,\mathrm{Hz}}$, $\gamma_2 = \frac{\gamma}{10^2}$. For the case considered the numerical values of N_p are shown in Fig. 4 (diamonds). Here it is taken that $\xi-\alpha = 7.2°$, which is the average over the values obtained from RVM-fits at the frequencies 1.71, 4.85 and 10.55 GHz (von Hoensbroech & Xilouris 1997); $P = 0.156$ s; $\gamma_2 = 1$. Using N_p and z_p, one can estimate the emission altitude z_0 assuming that $\omega = \omega_p(z_0)\sqrt{\gamma} = \omega_p(z_p)(z_0/z_p)^{-3}\sqrt{\gamma}$:

$$z_0/r_L = 6.83\times10^{-3} N_p^{1/3}\gamma_2^{1/3}\nu_9^{-2/3}\rho/C.$$

The results are shown in Fig. 4 by circles. One can see that the emission altitude lies within ∼2–4% of the light cylinder. This is in a good agreement with the estimate of z_0 found by von Hoensbroech & Xilouris (1997) in an alternative way. Based on polarization profile of PSR B0355+54 at 4.85 GHz of these authors obtained $z_0 = 214 \pm 120$ km, which can be reduced to the form $z_0/r_L = (2.74\pm1.54)\times10^{-2}$. Whether OPMs are generated by independent emission mechanisms or the extraordinary wave arises as a result of partial conversion of the ordinary one, the two modes are believed to originate at distances $\sim z_0$. As can be seen from Fig. 4, our implicit assumption that $z_0 \ll z_p$ is roughly appropriate.

In view of the continuity of the plasma flow within the open field line tube, it is convenient to introduce the multiplicity factor of the plasma along a fixed field line,

$$\kappa = \frac{NPce}{B}.$$

In terms of the quantities at the polarization-limiting radius, it is estimated as

$$\kappa = 1.875\left(\frac{z_p}{r_L}\right)^3 P^4 B_{\star_{12}}^{-1} N_p, \quad (9)$$

where $B_\star$ is the magnetic field strength at the neutron star surface, $B_{\star_{12}} = \frac{B_\star}{10^{12}\,\mathrm{G}}$, and the stellar radius is taken to be 10^6 cm.

The polar angle of the ray trajectory in the open field line tube, χ, can be expressed in terms of pulse phase of the ray along with parameters of observational geometry. One can notice that far from the emission region the radius-vector of the ray trajectory makes approximately the same angle with the magnetic axis as does the wavevector, $\chi \approx \theta_a$, where $\cos\theta_a = \cos\alpha\cos\xi + \sin\alpha\sin\xi\cos(\Phi + z/r_L)$. Hence, at the polarization-limiting radius, z_p, the polar angle reads:

$$\chi_p = |\xi-\alpha|\sqrt{1+(\eta+\rho)^2}. \quad (10)$$

For a given field line of the dipolar magnetic field $\chi = \chi_p\sqrt{z/z_p}$. This can be conveniently normalized to the polar angle of the last open field line, χ_f, to exclude the altitude z:

$$\chi/\chi_f = \chi_p\sqrt{C/\rho}. \quad (11)$$

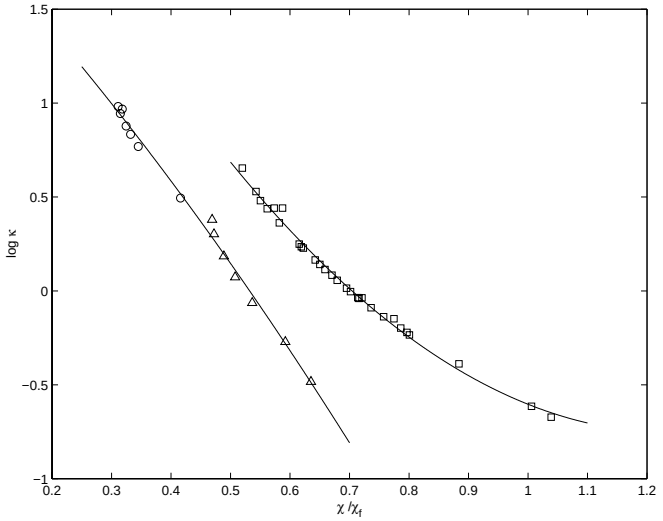

Fig. 5. Plasma density profiles of PSR B0355+54 (squares) and PSR B0628-28 (triangles and circles for the polarization data at 0.408 and 0.61 GHz, respectively).

The dependence $\kappa(\chi/\chi_f)$ presents the plasma density profile in the open field line tube. Although far from the emission region, at $z \sim z_p$, the tube is much wider than the radio beam, it is still possible to probe the plasma density over a substantial part of the tube. The point is that the polarization-limiting radius can vary considerably across the pulse profile (e.g., as in case of PSR B0355+54, see Fig. 4); then, because of the magnetosphere rotation, for different rays χ_p can differ markedly (cf. Eq. (10)) and, in addition, for distinct values of z_p even close values of χ_p may correspond to distant field lines (cf. Eq. (11)).

Strictly speaking, the rays observed at different pulse longitudes pass through the polarization-limiting region at different azimuths, so that the plasma is probed only along the line $\chi_p = \chi_p(\varphi_p)$. However, if the azimuthal density gradient is insignificant, one can suppose that $\kappa(\chi/\chi_f)$ completely describes the plasma density distribution, i.e. yields the density in any cross-section of the tube.

Substituting the calculated values of η and ρ into Eqs. (8)–(11), we find the plasma density profile of PSR B0355+54 (squares in Fig. 5). Here it is taken that $\log B_{\star_{12}} = -0.08$. The dependence $\kappa(\chi/\chi_f)$ exhibits a perfect exponential behaviour, with the exponent being well fitted by polynomial of the second order. The values of the multiplicity factor appear to be compatible with those given by modern theories of pair cascade, $\kappa \sim 1$–100 (e.g. Hibschman & Arons 2001a,b; Arendt & Eilek 2002). At the same time, strong nonuniformity of the plasma distribution across the tube is an essentially new result awaiting theoretical explanation.

The suggested technique of plasma diagnostics has also been applied to the polarization profiles of PSR B0628-28 at 0.408 and 0.61 GHz first published by Gould & Lyne (1998). The absence of orthogonal transitions over a broad frequency range (Suleymanova & Pugachev 2002) allows one to suppose that the average profiles of PSR B0628-28 are appropriate for our treatment. The resultant density profile is shown in Fig. 5 by triangles (0.408 GHz) and circles (0.61 GHz) (it is taken that

$\xi - \alpha = 3.7^\circ$ (Lyne & Manchester 1988), $\gamma_2 = 1$; $P = 1.244$ s, $\log B_{\star_{12}} = 0.48$). One can see that the polarization data at different frequencies lead to such multiplicity factors which lie on the same curve, testifying to the validity of the suggested technique. At the same time, this demonstrates that the multifrequency polarization studies can extend the region suitable for plasma probing, since the polarization-limiting radius is frequency-dependent. Indeed, as the rays reach $z_{\rm p}(\nu)$, the magnetosphere turns at an angle $\sim\frac{z_{\rm p}(\nu)}{r_{\rm L}}$, so that the rays of different frequencies observed at the same pulse longitudes probe the plasma at different field lines.

In the case of PSR B0628-28, the plasma multiplicity factor also shows an exponential decrease, however, in contrast to the density profile of PSR B0355+54, the second derivative of the exponent is ≤ 0, hinting at a flat maximum at smaller polar angles. Note that in both density profiles, the main uncertainty comes from the assumed values of $\xi - \alpha$. As has already been mentioned above, the customary RVM-fits usually yield questionable results. Therefore the density profiles obtained perhaps appear considerably shifted as a whole along both axes, though the characteristic exponential form of $\kappa(\chi/\chi_{\rm f})$ should remain unaltered. The multiplicity factors derived are also dependent on the assumed value of the characteristic Lorentz-factor of the plasma particles (cf. Eqs. (8) and (9)). Different models of the pair cascade certainly yield distinct distribution functions of the secondary plasma and therefore the characteristic Lorentz-factor should somewhat vary. However, γ is believed to be merely a scaling factor constant throughout the pulse profile for a pulsar, so that the shape of the density profile and its pulse-to-pulse variations are not affected.

4. Discussion and conclusions

We have developed a technique of density diagnostics of pulsar plasma based on polarization data. The natural waves which propagate through the plasma of the rotating magnetosphere should suffer PLE. As a result, the original linearly polarized waves acquire some circular polarization, v_m, and a shift in the PA of linear polarization, $\Delta\psi$. Separating the consequences of PLE from the observed polarization data makes it possible to reconstruct the plasma number density in the polarization-limiting region and, making use of the continuity of the plasma flow, to describe the plasma density distribution in a substantial part of the open field line tube.

The polarization profile of a pulsar at a fixed frequency typically does not allow one to reproduce the whole plasma density profile. Firstly, the rays propagating close enough to the magnetic axis remain invisible because of observational geometry. Secondly, far from the pulse profile peaks both V and L are too small to give reliable values of v_m. Thirdly, the asymmetry of the observed total-intensity profiles may hint at a marked azimuthal dependence of the plasma density, in which case the polarization profile yields the multiplicity factor only along a line in the transverse cross-section of the tube. Note that joint observations at different frequencies can enlarge the region suitable for the plasma diagnostics, since the polarization-limiting radius is frequency-dependent.

The technique of plasma diagnostics has been applied to the average polarization profiles of PSR B0355+54 at 4.85 GHz and PSR B0628-28 at 0.408 and 0.61 GHz. The resultant multiplicity factors are compatible with those predicted by the modern theories of electron-positron cascade. In addition, we have found that the density distribution across the tube is essentially nonuniform, exhibiting a perfect exponential decrease towards the tube edge.

Since we have used the average polarization profiles in place of the singe-pulse ones, the results are expected to be rough. At the same time, they demonstrate the possibilities of the technique suggested and urge its further application to the single-pulse data. With the present level of observational facilities, it seems realistic to obtain the instanteneous plasma density profiles for a number of pulsars.

The plasma multiplicities and their variability, which is believed to underlie polarization fluctuations in single pulses, can impose constraints on the models of pair cascade and stimulate more detailed theoretical studies of the physics of the polar gap. Furthermore, explicit knowledge of the structure of the secondary plasma flow may provide new insights into emission physics of pulsars. At first, it would be interesting to compare the profiles of total intensity and plasma density as well as their temporal variations. In particular, the plasma diagnostics can help to find out whether the drifting and nulling phenomena are indeed associated with the spatial and temporal changes in the plasma density. A rigorous description of the density distribution of pulsar plasma can also provide a basis for quantitative studies of the propagation effects. For example, observational evidence for a non-uniformity of the plasma distribution across the tube confirms that refraction should be mainly determined by a transverse rather than radial density gradient, since the transverse scale length of the tube is much less. This strongly supports our model of refraction (see e.g. Petrova & Lyubarskii 2000), where the transverse density gradient was merely postulated. At the same time, the results of the present paper testify against the alternative model of refraction (e.g. McKinnon 1997) based on 'ducted' propagation of subluminal waves along the magnetic lines, since in the presence of a significant transverse density gradient this regime should be broken (Barnard & Arons 1986).

On the whole, the technique of plasma diagnostics suggested in the present paper can become a useful tool for studying the physics of the pulsar magnetosphere.

Acknowledgements. This research has made use of the polarization profiles from the database of the European Pulsar Network, which is operated by Max-Plank Institut fur Radioastronomie. I am grateful to the referee, A. Jessner, for useful comments and suggestions.

References

Arendt, P. N. Jr., & Eilek, J. A. 2002, ApJ, 581, 451
Barnard, J. J. 1986, ApJ, 303, 280
Barnard, J. J., & Arons, J. 1986, ApJ, 302, 138
Cheng, A. F., & Ruderman, M. A. 1979, ApJ, 229, 348
Everett, J. E., & Weisberg, J. M. 2001, ApJ, 553, 341
Gil, J. A., Snakowski, J. A., & Stinebring, D. R. 1991, A&A, 242, 119
Gil, J. A., Lyne, A. G., & Rankin, J. M., et al. 1992, A&A, 255, 181

Gould, D. M., & Lyne, A. G. 1998, MNRAS, 301, 235
Hibschman, J. A., & Arons, J. 2001a, ApJ, 554, 624
Hibschman, J. A., & Arons, J. 2001b, ApJ, 560, 871
Lyne, A. G., & Manchester, R. N. 1988, MNRAS, 234, 477
Lyubarskii, Yu. E. 1996, A&A, 308, 809
Lyubarskii, Yu. E., & Petrova, S. A. 1999, Ap&SS, 262, 379
Manchester, R. N., & Taylor, J. H. 1977, Pulsars (San Francisco: W. H. Freeman and Company)
McKinnon, M. M. 1997, ApJ, 475, 763
McKinnon, M. M. 2002, ApJ, 568, 302
McKinnon, M. M., & Stinebring, D. R. 1998, ApJ, 502, 883
McKinnon, M. M., & Stinebring, D. R. 2000, ApJ, 529, 435
Petrova, S. A. 2001, A&A, 378, 883
Petrova, S. A., & Lyubarskii, Yu. E. 2000, A&A, 355, 1168
Stinebring, D. R. 1982, Ph.D. Thesis, Cornell University
Suleymanova, S. A., & Pugachev, V. D. 2002, AZh, 79, 345
von Hoensbroech, A., & Xilouris, K. M. 1997, A&AS, 126, 121
Xilouris, K. M., Sieradakis, J. H., Gil, J. A., et al. 1995, A&A, 293, 153